

Pair correlation function for spin glasses

Julio F. Fernández^{1,2,*} and Juan J. Alonso³

¹*Departamento de Física de la Materia Condensada, Universidad de Zaragoza, 50009 Zaragoza, Spain*

²*Instituto Carlos I de Física Teórica y Computacional, Universidad de Granada, 18071 Granada, Spain*

³*Física Aplicada I, Universidad de Málaga, 29071 Málaga, Spain*

(Received 13 June 2012; published 9 October 2012)

We extract a pair correlation function (PCF) from probability distributions of the spin-overlap parameter q . The distributions come from Monte Carlo simulations. A measure, w , of the thermal fluctuations of magnetic patterns follows from the PCFs. We also obtain rms deviations (over different system samples) δp away from average probabilities for q . For the linear system sizes L that we have studied, w and δp are independent of L in the Edwards-Anderson model but scale as $1/L$ and \sqrt{L} , respectively, in the Sherrington-Kirkpatrick model.

DOI: [10.1103/PhysRevB.86.140402](https://doi.org/10.1103/PhysRevB.86.140402)

PACS number(s): 75.10.Nr, 75.30.Kz, 75.40.Mg, 75.50.Lk

1. Introduction. After decades of much work, the nature of the spin-glass (SG) phase is still unclear. A SG phase is found at low temperature in magnetic systems which are both *quenched disordered* and *frustrated*.^{1,2} Random spin positions as well as random spin-spin couplings are sources of quenched disorder. When competition arises, because not all spin-spin coupling energies can be minimized simultaneously, a system is said to be *frustrated*.³ Fixed disorder and built-in competition are the two essential ingredients of *complex* systems.⁴

The Sherrington-Kirkpatrick (SK) spin-glass model,⁵ in which each spin-spin coupling is assigned at random, without regard to spin-spin distance, is quenched disordered and frustrated. Its exact solution^{1,6-8} implies that different random number seeds (which fully specify all couplings) can give rise, in thermal equilibrium, to magnetic patterns which are macroscopically different.⁹ Diversity of macroscopic observable magnitudes arising from random arrangements of microscopic constituents is the hallmark of complexity.^{10,11}

However, no consensus has yet been reached on whether the *macroscopic* limit of the Edwards-Anderson¹² (EA) model, in which only nearest-neighbor spins interact, (i) follows closely the SK model,¹³ (ii) deviates from SK model behavior but nevertheless shows some diversity,¹⁴ or (iii) fits a radically different picture, the droplet scenario,^{15,16} in which SGs with up-down symmetry can only be found in one of two macroscopic spin configurations which are related by global spin inversion. (See also Ref. 17.) Thus, according to the droplet theory, the two necessary ingredients (quenched disorder and frustration) for complexity would become unable to generate diversity in the macroscopic limit of EA systems.

Complexity would make SGs rather exceptional among the many-particle systems of statistical physics. On the other hand, they would share this property with systems one finds elsewhere, such as in the life sciences,¹⁸ information systems,¹⁹ optimization problems,²⁰ and finance.²¹ In every one of these fields complexity and diversity are the rule rather than the exception. Thus, addressing these issues in SGs with standard methods of statistical physics can lead to insight into other seemingly disconnected areas of research.

The basic tool for the characterization of the SG state is the spin overlap q between two system states.¹ To define it, let $\sigma_i^{(1)}$ be the spin of system state 1 at site i , and similarly for 2. Then, $q \equiv N^{-1} \sum_i \sigma_i^{(1)} \sigma_i^{(2)}$; i.e., q is the average (over all sites) spin

alignment between states 1 and 2. One usually lets states 1 and 2 be either (i) of a given time evolution of a given specimen at two widely different times,²² or (ii) of two independent (1 and 2) time evolutions of the same specimen. For numerical work, we follow the latter of the two procedures.

In macroscopic SK systems, the probability density, $p(q)$, averaged over all realizations of quenched disorder (RQD), fulfills^{1,8} (i) $p(q) \propto f(q) + \delta(q - q_m)$ for $q \geq 0$, where $f(q)$ is a smooth function of q for $q < q_m$ and $f(q) = 0$ for $q \geq q_m$, and (ii) $p(q) = p(-q)$ if no magnetic field is applied (which we will assume throughout).

The fact that $f(q) \neq 0$ in the SK model implies the existence of “odd” magnetic patterns (in addition to a pair of ordinary magnetic patterns that one expects to observe in all magnetic systems), whence complexity follows. Understandably, attempts at discerning between the macroscopic behaviors of the SK and EA models have focused on $p(q)$.

Specific system samples are interesting to examine. At least for *finite-size* EA systems, seed-dependent spin configurations do appear,²³ much as in the SK model,²⁴ in thermal equilibrium. This is illustrated in Figs. 1(a) and 1(b) of Ref. 25, where plots of $p_{\mathcal{J}}(q)$ vs q are shown for two different \mathcal{J} sets of spin-spin couplings. Whereas some portions of $p_{\mathcal{J}}(q)$ differ drastically from Figs. 1(a) to 1(b) of Ref. 25, the portions for larger values of q are alike and all of them peak near $q = q_m$. We let *self-overlap* spikes (SOS) stand for spikes centered near q_m . Because they are all centered near the same position, the average of SOS (one for each RQD) over all RQD gives rise to the large peak at $q = q_m$ in Fig. 1(c) of Ref. 25. Spikes centered on smaller q values, which vary randomly with different RQD, come from spin overlaps between states that belong to different basins of attraction. Accordingly, we refer to them as *cross-overlap* spikes (COS).

Interesting as it might be, no statistical information on spikes, except for a very recent report,²⁶ has been available. Very little information on COS follows from the (average) behavior of $p(q)$. Cross-over spike statistics would enrich our picture of the SG state, somewhat as the pair correlation function does for the physics of liquids.

We aim to show how COS in $p_{\mathcal{J}}(q)$, such as the ones shown in Fig. 1(b) of Ref. 25, of which the locations and shapes vary randomly over different RQD, can be added in a coherent fashion, in order to obtain a pair correlation function,

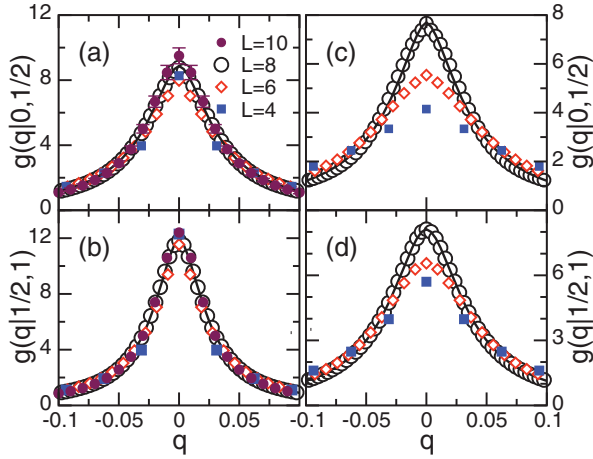


FIG. 1. (Color online) (a) Plots of $g(q | 0, 1/2)$ vs q for EA systems at $T = 0.2$, with the values of L shown. The full line is for a fit to the $L = 8$ data points with $\Gamma^\nu/[w(\Gamma^\nu + |q|^\nu)]$. (b) Same as for (a) but for $g(q | 1/2, 1)$. (c) Same as for (a) but for the SK model. (d) Same as for (a) but for $g(q | 1/2, 1)$ for the SK model. Values of w and Γ are given in Fig. 2 for all T and L above, in both the EA and SK models. Values for ν are given in the text.

$g(q | 0, Q)$, which is an average (in a sense which is defined below) over all RQD of all COS in the $0 < q < Q$ range. We also (numerically) calculate the width of $g(q | 0, Q)$, which is a measure of magnetic pattern thermal fluctuations, for $Q = 1/2$. The results we obtain for low temperature (T) point to the following behavior: (i) $g(q | 0, 1/2)$ closely follows a Lévy-flight-like distribution,²⁸ (ii) the pair correlation functions that follow from SOS and COS are roughly equal, that is, $g(q | 0, 1/2) \approx g(q | 1/2, 1)$, and (iii) the width of $g(q | 0, 1/2)$ varies little, if at all, with linear system size L (scales as $1/L$) in the EA (SK) model. Thus, different ranges of spin-spin interaction give rise to qualitative differences between the complex behavior of spin glasses.

2. Models. We study the SK and EA models. In both of them, a $\sigma_i = \pm 1$ spin is located at each i th site of a simple cubic lattice of $N = L^3$ sites. The interaction energy between a pair of spins at sites i and j is given by $J_{ij}\sigma_i\sigma_j$. We let $J_{ij} = \pm 1/\sqrt{N}$ randomly, without bias, for all ij site pairs in the SK model. The transition temperature T_{sg} between the paramagnetic and SG phase is $T_{sg} = 1$.^{1,5} For the EA model, $J_{ij} = 0$ unless ij are nearest-neighbor pairs, and we draw each nearest-neighbor bond J_{ij} independently from unbiased Gaussian distributions of unit variance. Then, $T_{sg} \simeq 0.95$.²⁹

We let $\langle u_{\mathcal{J}} \rangle_{\mathcal{J}}$ stand for the average of a thermal equilibrium quantity $u_{\mathcal{J}}$ over a number N_s of different sets of random bonds $\{\mathcal{J}\}$.

3. Pair correlation function. Aiming for statistical information on COS at low temperature, we let

$$G_{\mathcal{J}}(q | Q_1, Q_2) = \int_{Q_1+h(-q)}^{Q_2-h(q)} dq_1 p_{\mathcal{J}}(q_1) p_{\mathcal{J}}(q_1 + q), \quad (1)$$

where $h(q) = 0$ if $q < 0$ and $h(q) = q$ if $q \geq 0$. Clearly, $(\Delta Q - |q|)^{-1} G_{\mathcal{J}}(q | Q_1, Q_2)$, where $\Delta Q = Q_2 - Q_1$, is the average of $p_{\mathcal{J}}(q_1) p_{\mathcal{J}}(q_1 + q)$ over the $(Q_1 + h(-q), Q_2 - h(q))$ domain. We term $G(q | Q_1, Q_2) \equiv \langle G_{\mathcal{J}}(q | Q_1, Q_2) \rangle_{\mathcal{J}}$ the *pair correlation function*.

The integral in Eq. (1) is as for the probability density to be at $-q$ after a two-step random walk which starts at the origin, in which the *length* of both steps is identically distributed, but they are taken in opposite directions. Note that $G_{\mathcal{J}}(q | Q_1, Q_2)$ (i) peaks at $q = 0$,³⁰ (ii) is even with respect to $q = 0$, since $p_{\mathcal{J}}(q) = p_{\mathcal{J}}(-q)$, and (iii) is somewhat broader than $p_{\mathcal{J}}(q)$ (from the theory of random walks).

The operation defined in Eq. (1) clearly displaces to $q = 0$ any spike in $p_{\mathcal{J}}$ within the (Q_1, Q_2) domain. Thus, by appropriate choice of Q_1 and Q_2 values, $G(q | Q_1, Q_2)$ enables one to make comparisons (see below) *on equal footing* of statistical information on SOS and COS.

We can also define $g(q | Q_1, Q_2) = BG(q | Q_1, Q_2)$, where $B \equiv 1/\int_{Q_1-Q_2}^{Q_2-Q_1} dq G(q | Q_1, Q_2)$. One can think of $g(q | Q_1, Q_2)$ as the (conditional) probability density that $q_2 - q_1 = q$, given that $q_1, q_2 \in (Q_1, Q_2)$: Read q_1 and q_2 at infinitely far apart times from an identical pair of systems which evolve independently in time while in equilibrium; now, register the value q , given by $q_2 - q_1$ if $q_1, q_2 \in (Q_1, Q_2)$, but not otherwise; repeat the procedure indefinitely with different pairs of identical samples. The probability density for q taken from all the registered q values is $g(q | Q_1, Q_2)$.

We define widths of two correlation functions. For a distribution function $F(x)$ such that $\int_{-\infty}^{\infty} dx xF(x) = 0$, it makes sense to define a width δx by $\delta x F(0) \equiv \int_{-\infty}^{\infty} dx F(x)$. Since $g(q | Q_1, Q_2)$ is normalized, we let

$$w(Q_1, Q_2) = 1/g(0 | Q_1, Q_2). \quad (2)$$

For short, we let $w_+ \equiv w(0, 1/2)$, $w_- \equiv w(1/2, 1)$. For $T \lesssim 0.3$, w_- and w_+ are widths for COS and SOS, respectively. Furthermore, note (i) $g(q | Q_1, Q_2) \leq g(0 | Q_1, Q_2)$ implies $w_-, w_+ \leq 1/2$, (ii) that we can think of w_- as an intrinsic width of $g(q | 0, 1/2)$, if $w_- \ll 1/2$, and similarly for w_+ . We also define half-widths at half-maxima Γ_- and Γ_+ by $2g(\Gamma_- | 0, 1/2) = g(0 | 0, 1/2)$ and $2g(\Gamma_+ | 1/2, 1) = g(0 | 1/2, 1)$.

4. Method. All numerical results given below follow from parallel tempered Monte Carlo (MC) simulations.³¹⁻³³ We give all times in terms of MC sweeps.

All pairs of systems start running from independent random spin configurations. Each system pair is then allowed to come, in time τ_s , to equilibrium with each reservoir of a string of them at T , $T + \Delta T$, $T + 2\Delta T$, \dots , before readings of q values are taken over an additional τ_s time span. From many such readings, the thermal equilibrium probability $p_{\mathcal{J}}(q)$, for a given RQD, is obtained for each temperature. Relevant simulation parameters are in Table I.

We next consider equilibration. Let $X_n(Q) = \int_{-Q}^Q dq p_{\mathcal{J}}(q)$ for the n th sample. Furthermore, let $\Omega_Q(k) = \sum_{n=1}^k X_n(Q)$. Note that both the average value of $p(q)$, as well as deviations from it, over $q \in (-Q, Q)$, follow from $\Omega_Q(k)$ for a sufficiently large k . Plots of Ω_Q vs k are shown in Fig. 2 of Ref. 27 for $L = 8$. Similar plots for $4 \leq L \leq 10$ are unchanged as τ_s increases beyond the values given in Table I. From such considerations, we infer that *equilibrium* values of $\Omega_Q(k)$ follow from MC runs after equilibrating for some $10^{2+L/2}$ MC sweeps.

5. Results. Data points for the pair correlation function are shown in Fig. 1 for $T = 0.2$. The two graphs on the left-hand side (right-hand side) are for the EA (SK) model. The two top

TABLE I. Number of samples N_s and equilibration time τ_s , as well as time for subsequent averaging. Average acceptance rates for system configuration exchanges at all T are larger than A , and ΔT is the temperature spacing between systems in the tempered MC setup.

L	SK			EA				L	SK			EA			
	4	6	8	4	6	8	10		4	6	8	4	6	8	10
$\tau_s/10^4$	5	5	10	1	10	10^2	10^3	$10A$	7	5	4	7	4	5	4.5
$N_s/10^4$	2	1	1	3	4	3	0.5	$10^2\Delta T$	4	4	4	10	10	5	4

(bottom) graphs are for $Q_1, Q_2 = 0, 1/2$ ($Q_1, Q_2 = 1/2, 1$), which, since for $T \lesssim 0.3$, are for COS (SOS). While neither COS nor SOS exhibit significant size dependence in the EA model, they clearly do so in the SK model. We return to this point below.

All curves shown in Fig. 1 are rather pointed at the top. This is in contrast with the well-known curves for $p(q)$ in the neighborhood of $q = q_m$ for finite SK systems³⁴ [but see Ref. 24 for some $p_{\mathcal{J}}(q)$]. This is because values of q_m vary over different RQD by amounts which, at least for $L = 8$ and $T \lesssim 0.3$, are roughly equal to Γ_+ for the SK model. Thus, averaging $p_{\mathcal{J}}(q)$ over all RQD gives rise to a rounded $p(q)$ while $g(q | 1/2, 1)$, being a *coherent*-like superposition of spikes over different RQD, reveals their individual shapes.

Good fits to all plots in Fig. 1 are provided by $\Gamma^\nu/[w(\Gamma^\nu + |q|^\nu)]$, which closely follows a Lévy flight distribution²⁸ for $1 < \nu \leq 2$. Fits to the $L = 8$ data are shown in Figs. 1(a)–1(c), and 1(d). For both the EA and SK models, $\nu \simeq 2(1 - 1/L)$ for all $T \lesssim 0.3$. Values for w and Γ are given in all panels of Fig. 2. As in Fig. 1, the two graphs on the left-hand side (right-hand side) are for the EA (SK) model. The two top (bottom) graphs are for $Q_1, Q_2 = 0, 1/2$ ($Q_1, Q_2 = 1/2, 1$), which for $T \lesssim 0.4$ are for COS (SOS).

We also note that if $z = x_1 + x_2$, and x_1 and x_2 are drawn from a Lévy flight distribution, then, within a few percent, in obvious notation, $\Gamma_z \simeq \Gamma_x 2/\sqrt{\gamma - 1}$ if $1.15 \lesssim \gamma \leq 2$. Thus, $g(q | Q_1, Q_2)$ is approximately $2/\sqrt{\gamma - 1}$ times wider than spikes in the (Q_1, Q_2) domain.

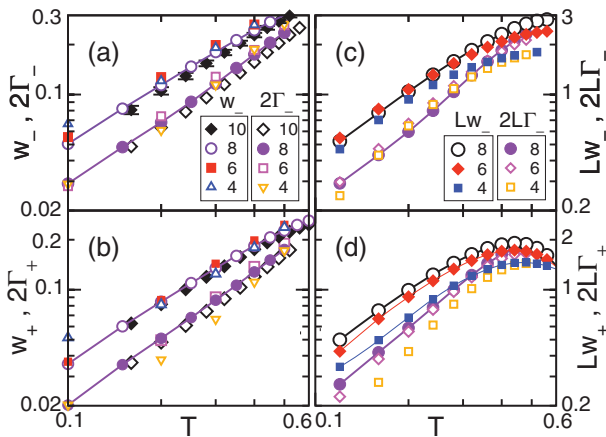


FIG. 2. (Color online) (a) Log-log plots of w_- and $2\Gamma_-$ vs T , for EA systems of $L = 4, 6, 8$ and $L = 10$, as shown. Error bars for $L = 10$ are shown, but for smaller L values they are hidden by symbols. (b) Same as in (a) but for w_+ and $2\Gamma_+$. (c) Same as in (a) but for SK systems of $L = 4, 6$ and $L = 8$, as shown. (d) Same as in (c) but for Lw_+ and $2L\Gamma_+$.

Widths w_- and w_+ appear in Figs. 2(a) and 2(b) to be size independent for $0 < T \lesssim 0.3$. This points to finite widths for COS and SOS in the $L \rightarrow \infty$ limit of the EA model at low temperature. On the other hand, $w_-, w_+ \sim 1/L$ for large L in the SK model seems consistent with the data points shown in Figs. 2(c) and 2(d) for w_- and w_+ .³⁵

Results for probability fluctuations over different RQD are next given. Additional information follows from the (unnormalized) pair correlation function $G(q | Q_1, Q_2)$. For instance,

$$G(0 | 0, Q) = Q[(\bar{p}^Q)^2 + (\overline{\delta p^Q})^2], \quad (3)$$

where \bar{p}^Q and $(\overline{\delta p^Q})^2$ are the averages of $p(q)$ and $[\delta p(q)]^2$ over the $0 < |q| < Q$ range, respectively, and $\delta p(q)$ is the rms deviation of $p_{\mathcal{J}}(q)$ from $p(q)$ over all RQD. Plots of $(\overline{\delta p^Q})^2$ vs T for $Q = 1/2$ and various systems sizes of the EA and SK models are shown in Fig. 3. These plots do not vary with Q , at least down to $Q = 1/8$. Note that whereas $(\overline{\delta p^Q})^2$ scales as $\sim \sqrt{L}$ in the SK model, it appears to be, within statistical errors, independent of L in the EA model.

The rms deviation of $X_{\mathcal{J}}(Q)$ from $\langle X_{\mathcal{J}}(Q) \rangle$ differs qualitatively from $(\overline{\delta p^Q})^2$ if Q is not too small. This is because

$$\langle X_{\mathcal{J}}^2(Q) \rangle_{\mathcal{J}} = w(0, Q)Q[(\bar{p}^Q)^2 + (\overline{\delta p^Q})^2], \quad (4)$$

as follows from Eq. (2). Quantity $\langle X_{\mathcal{J}}^2(Q) \rangle_{\mathcal{J}}$ is examined in some detail in Ref. 37, where it is termed X_2 . Now, $w(0, Q)$ and $(\overline{\delta p^Q})^2$ come into $\langle X_{\mathcal{J}}^2(Q) \rangle_{\mathcal{J}}$ as a product, which happens to be size independent not only in the EA model [where both $w(0, Q)$ and $(\overline{\delta p^Q})^2$ are size independent] but in the SK model as well if $Q \gg w(0, Q)$, since $w(0, Q) \sim 1/L$ then and $(\overline{\delta p^Q})^2 \sim L$. For the neighborhood of $X_1 = 0$ in the second panel of Fig. 2 of Ref. 37, things are quite different. Then, $Q \gg w(0, Q)$ is no longer fulfilled [$w(0, Q) \approx Q$ in both the EA and SK model

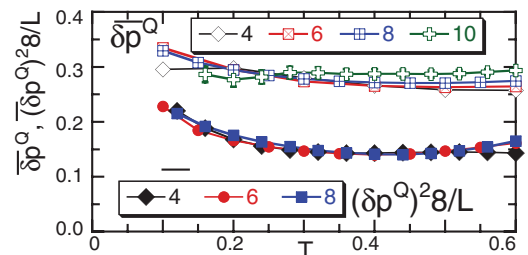


FIG. 3. (Color online) Plots of $(\overline{\delta p^Q})^2$ and of $(\overline{\delta p^Q})^2 8/L$ vs T for the EA and SK models, respectively, $Q = 1/2$, and the values of L shown. Except for $L = 10$, icons cover all error bars.

then], and [see Eq. (4)] X_2/X_1 do exhibit size effects then. Our own plots (not shown) of X_2/X_1 vs X_1 for $T = 0.2$ and $Q = 1/2$ show size effects we expect for the SK model [i.e., X_2/X_1 moves towards the mean-field line as $L \rightarrow \infty$ and $w(0, Q)$ consequently becomes smaller]. Slight size effects are seen in Ref. 37 for the EA model at $T = 0.6$, but there are no appreciable size effects in our own plots (not shown) at $T = 0.2$.

6. *Conclusions.* We have given a recipe for a coherent addition of self- and cross-overlap spikes (SOS and COS). The latter are centered on positions that vary randomly with RQD. In both the EA and SK models, the correlation functions for SOS and COS turn out to be approximately equal. The widths w_- and Γ_- (both for COS) give a measure of the thermal fluctuations of magnetic patterns. They are not too different from w_+ and Γ_+ (both for SOS), respectively. Neither w_{\pm} nor Γ_{\pm} vary much with linear system size L in the EA model but scale approximately as $1/L$ in the SK model. Their variation with system size at low temperature suggests they vanish in

the macroscopic limit of the SK model but remain finite in the EA model. Finally, $\overline{\delta p}^Q$ does not vary much with L in the EA model but scales as $L^{1/2}$ in the SK model.³⁶ Our results may be compared with mean-field predictions, that $\overline{\delta p}^Q \rightarrow \infty$ as $L \rightarrow \infty$ for any $Q > 0$.³⁸

The rule we have uncovered—which relates thermal fluctuations of magnetic patterns as well as probability fluctuations to interaction range—may well be valid in some broader domain, beyond the SK and EA models. For one, preliminary (unpublished) work yields similar results for some *spatially* disordered systems which are geometrically frustrated. Extensions to other fields of complex systems easily come to mind.

Acknowledgments. We are grateful to L. Falvello, M. A. Moore, and D. Sherrington for insightful remarks. We thank SCBI and LMN, both at Universidad de Málaga, for much computer time. Grant No. FIS2009-08451 from the Ministerio de Economía y Competitividad of Spain is gratefully acknowledged.

*jefe@unizar.es

¹M. Mézard, G. Parisi, and M. Virasoro, *Spin Glass Theory and Beyond* (World Scientific, Singapore, 2004).

²G. Aeppli and P. Chandra, *Science* **275**, 177 (1997).

³The importance of frustration in SGs was first brought out in G. Toulouse, *Comm. Phys.* **2**, 115 (1977).

⁴S. E. Page, *Diversity and Complexity* (Princeton University Press, Princeton, 2010); for a wide variety of definitions of complexity, see S. Lloyd, *IEEE Cntr. Syst. Mag.* **21**, 7 (2001).

⁵D. Sherrington and S. Kirkpatrick, *Phys. Rev. Lett.* **32**, 1792 (1975).

⁶J. Thouless, P. W. Anderson, and R. Palmer, *Philos. Mag.* **35**, 593 (1977).

⁷A. J. Bray and M. A. Moore, *Phys. Rev. Lett.* **41**, 1068 (1978).

⁸G. Parisi, *Phys. Rev. Lett.* **43**, 1754 (1979).

⁹This was first shown to follow for the SK model in M. Mézard, G. Parisi, N. Sourlas, G. Toulouse, and M. Virasoro, *Phys. Rev. Lett.* **52**, 1156 (1984).

¹⁰This outlook follows after Parisi's view of complexity in biology, [arXiv:cond-mat/9412018](https://arxiv.org/abs/cond-mat/9412018).

¹¹For a *quantitative* definition of complexity in spin glasses, as well as further references, see, for instance, T. Aspelmeier, A. J. Bray, and M. A. Moore, *Phys. Rev. Lett.* **92**, 087203 (2004).

¹²S. F. Edwards and P. W. Anderson, *J. Phys. F* **5**, 965 (1975).

¹³P. Contucci, C. Giardinà, C. Giberti, G. Parisi, and C. Vernia, *Phys. Rev. Lett.* **99**, 057206 (2007); G. Parisi and F. Ricci-Tersenghi, *Philos. Mag.* **92**, 341 (2012).

¹⁴F. Krzakala and O. C. Martin, *Phys. Rev. Lett.* **85**, 3013 (2000); M. Palassini and A. P. Young, *ibid.* **85**, 3017 (2000); J. Houdayer and O. C. Martin, *Europhys. Lett.* **49**, 794 (2000); M. Palassini, F. Liers, M. Juenger, and A. P. Young, *Phys. Rev. B* **68**, 064413 (2003); G. Hed, A. P. Young, and E. Domany, *Phys. Rev. Lett.* **92**, 157201 (2004).

¹⁵D. S. Fisher and D. A. Huse, *Phys. Rev. B* **38**, 386 (1988); M. A. Moore and A. J. Bray, *J. Phys. C* **18**, L699 (1985); M. A. Moore, *J. Phys. A* **38**, L783 (2006).

¹⁶M. A. Moore, H. Bokil, and B. Drossel, *Phys. Rev. Lett.* **81**, 4252 (1998); **82**, 5177 (1999).

¹⁷C. M. Newman and D. L. Stein, *Phys. Rev. E* **57**, 1356 (1998).

¹⁸H. Fraunfelder, S. G. Sligar, and P. G. Wolynes, *Science* **254**, 1598 (1991).

¹⁹See, for instance, M. Garey and D. S. Johnson, *Computers and Intractability: A Guide to the Theory of NP-Completeness* (Freeman, San Francisco, 1979); N. Sourlas, *Nature (London)* **339**, 693 (1989); Y. Fu and P. W. Anderson, *J. Phys. A* **19**, 1605 (1986); M. Mézard and A. Montanari, *Information, Physics, and Computation* (Oxford Graduate Texts, Oxford, 2009); F. Ricci-Tersenghi, *Science* **330**, 1639 (2010); for management information systems, see, for instance, *The Oxford Handbook of Management Information Systems*, edited by R. D. Galliers and W. L. Currie (Oxford University Press, Oxford, 2011).

²⁰S. Kirkpatrick, C. D. Gelatt, and M. P. Vecchi, *Science* **220**, 671 (1983).

²¹N. F. Johnson, P. Jefferies, and P. M. Hui, *Financial Market Complexity* (Oxford University Press, Oxford, 2003).

²²How far apart, in order for all correlations between states 1 and 2 to be lost, is discussed in J. F. Fernández, *Phys. Rev. B* **82**, 144436 (2010).

²³E. Marinari, G. Parisi, and J. J. Ruiz-Lorenzo, *Phys. Rev. B* **58**, 14852 (1998).

²⁴For the SK model, see, for instance, Fig. 2 in T. Aspelmeier, A. Billoire, E. Marinari, and M. A. Moore, *J. Phys. A* **41**, 324008 (2008).

²⁵See Supplemental Material at <http://link.aps.org/supplemental/10.1103/PhysRevB.86.140402> for plots of $p_{\mathcal{J}}(q)$ vs q for two different \mathcal{J} sets of spin-spin couplings.

²⁶B. Yuceosoy, H. G. Katzgraber, and J. Machta, arXiv:1206.0783.

²⁷See Supplemental Material at <http://link.aps.org/supplemental/10.1103/PhysRevB.86.140402> for plots of Ω_Q , for $Q = 1/2$, vs the number k of EA sample systems.

²⁸R. N. Mantegna and H. E. Stanley, *Phys. Rev. Lett.* **73**, 2946 (1994); G. M. Zaslavsky, in *Lévy Flights and Related Topics in Physics*, edited by M. Shlesinger, G. Zaslavsky, and U. Frisch (Springer-Verlag, Heidelberg, 1995), p. 216.

- ²⁹H. G. Katzgraber, M. Körner, and A. P. Young, *Phys. Rev. B* **73**, 224432 (2006).
- ³⁰The fact that $G_{\mathcal{J}}(0 | Q_1, Q_2) \geq G_{\mathcal{J}}(q | Q_1, Q_2)$ follows easily from the inequality $(A - B)^2 \geq 0$, letting $A^2 = B^2 = \int dx f^2(x)$ and $AB = \int dx f(x)f(x+u)$.
- ³¹K. Hukushima and K. Nemoto, *J. Phys. Soc. Jpn.* **65**, 1604 (1996).
- ³²For a critique of parallel tempering, see, J. Machta, *Phys. Rev. E* **80**, 056706 (2009).
- ³³J. J. Alonso and J. F. Fernández, *Phys. Rev. B* **81**, 064408 (2010).
- ³⁴G. Parisi, F. Ritort, and F. Slanina, *J. Phys. A* **26**, 3775 (1993); A. Billoire, S. Franz, and E. Marinari, *ibid.* **36**, 15 (2003).
- ³⁵ $w_+ \sim 1/L$ for the SK model seems consistent with the behavior of $p(q)$ in the neighborhood of q_m shown in Ref. 34.
- ³⁶Data on spike heights given in Ref. 26 is complementary to ours and points in the same direction—that the macroscopic behavior of the EA and SK models is different.
- ³⁷R. A. Baños *et al.*, *Phys. Rev. B* **84**, 174209 (2011).
- ³⁸See Eq. (7) of Ref. 9.